Literature Seminar

F R E T

060913 Kenzo Yamatsugu (M2)

with a focus on organic and inroganic dyes

0. Introduction

Protein - Protein interaction, Protein - DNA interaction, Chemical Sensor and ....

⇩

We want to know physical relationships.

⇩

F R E T

Fluorescence Resonance Energy Transfer

+ Nonradiative process whereby an excitated state donor D transfers its energy to a proximal ground state acceptor A. (Figure.1)
+ The rate of energy transfer is **highly dependent on the distance "r"** between the donor and acceptor molecules.
+ By measuring the FRET efficiency, **we can know the distance** between donor and acceptor.
÷ spectroscopic **ruler**

Figure. 1 FRET

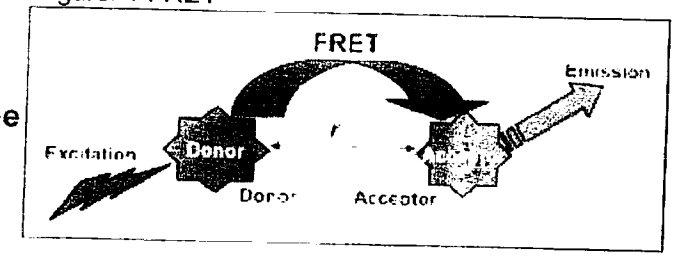

Figure. 2 Fluorophores

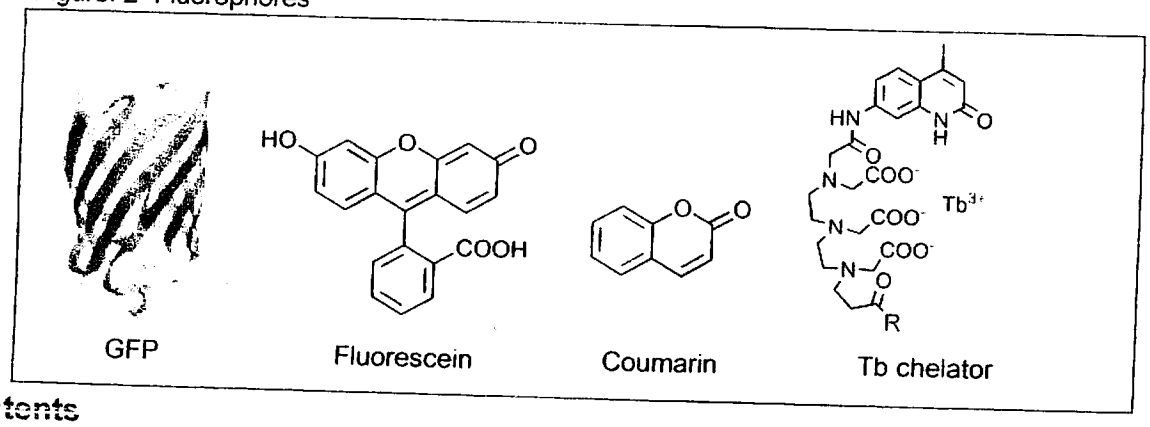

Contents

1. Features of FRET

2.1 Fluorescence, Stokes Shift, FRET : qualitative aspects

+ Stokes Shift
a phenomenon that emission wave length is longer than excitation wave length.

+ FRET
requirements are
1. large spectral overlap
2. distance (10 ~ 100Å)
3. appropriate dipole orientation (κ^2 is not zero.)

Figure. 3 Fluorescence

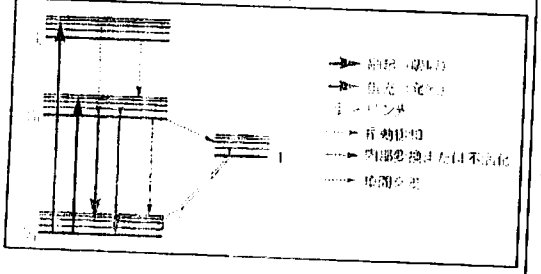

Figure.4 Stokes Shift and Spectral overlap between donor and acceptor

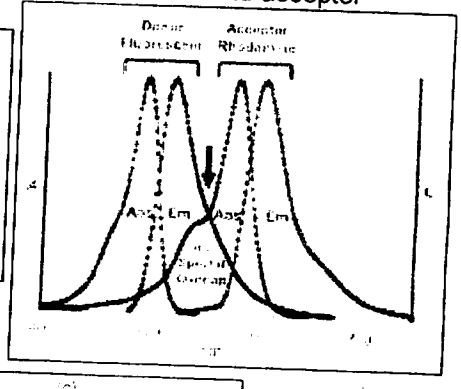

Figure. 5 Dipole orientation

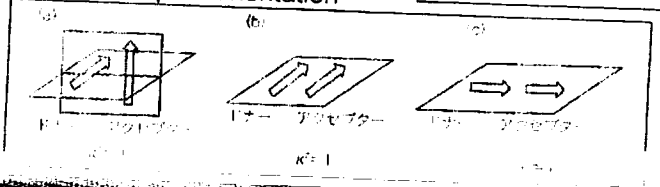

2.2 FRET : quantitative aspects

Förster : a person who established the quantitative theory on FRET in 1948. According to his theory,

$$E = R_0^6 / (R_0^6 + r^6)$$

$$\longrightarrow \quad r = R_0(1/E - 1)^{1/6} \qquad \text{eq. 1}$$

E = FRET efficiency, R_0 = Förster radius, r = distance beween donor and acceptor

R_0 is the distance between donor and acceptor at which 50% of the excited donor molecule decay by energy transfer. And R_0 is a constant which is inherent in the pair of donor and acceptor and their orientation.

$$R_0 = 9.78 \times 10^3[\kappa^2 n^{-4} Q_d J]^{1/6} \ (\text{in Å}) \qquad \text{eq. 2}$$

κ^2 = dipole orientation, n = refractive index of the medium, Q_d = quantum yield of donor, J = overlap integral in the absence of acceptor

On the other hand,

$$E = 1 - F_{da} / F_d \qquad \text{eq. 3}$$

F_{da} = Fluorescence intensity of donor in the presence of acceptor
F_d = Fluorescence intensity of donor in the absence of acceptor

⇩

R_0 : 計算可, E : 測定可 $\xrightarrow[\text{eq. 1}]{}$ r = 計算可

2. Design of FRET-based sensor : H_2O_2 sensor

2.0 design approach in general ref. C. J. Chang *et al. J. Am. Chem. Soc.* **2006**, *128*, 9640.

No FRET $\xrightarrow{\text{target}}$ FRET

in the absence of target — in the presence of target

\+ FRET
requirements are
1. large spectral overlap
2. distance (10 ~ 100Å)
3. appropriate dipole orientation (κ^2 is not zero.)

⇨ + Approach
in the absence of target ⟶ one of requirements is not met.
in the presence of target ⟶ all the requirements are met.

2.1 this work

Figure.6 Design of the H_2O_2 sensor

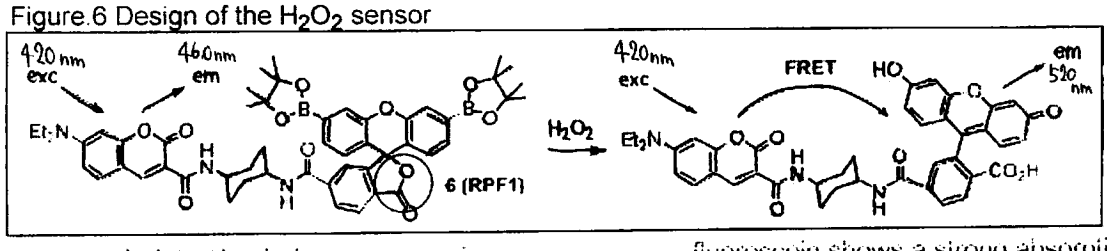

lactone form = spectral overlap between coumarin emission and fluorescein absorption is minimized

⇩

FRET is suppressed and only blue donor emission is observed upon excitation of the coumarin fluorophore

fluorescein shows a strong absorption in the coumarin emission region, then spectral overlap is enhanced

⇩

Excitation of the donor coumarin fluorophore results in increased green fluorescein acceptor emission by FRET

1. large spectral overlap

linker : *trans* 1,4 disubstituted cyclohexane ⟵ inspired by Nagano sensei's works
ref. T. Nagano *et al. J. Am. Chem. Soc.* **2002**, *124*, 1653.

Nagano-sensei's work = enzyme-cleavable sensor molecule for phosphodiesterase activity based on FRET

Figure. 7 CPF 4 : enzyme-cleavable sensor for phosphodiesterase I

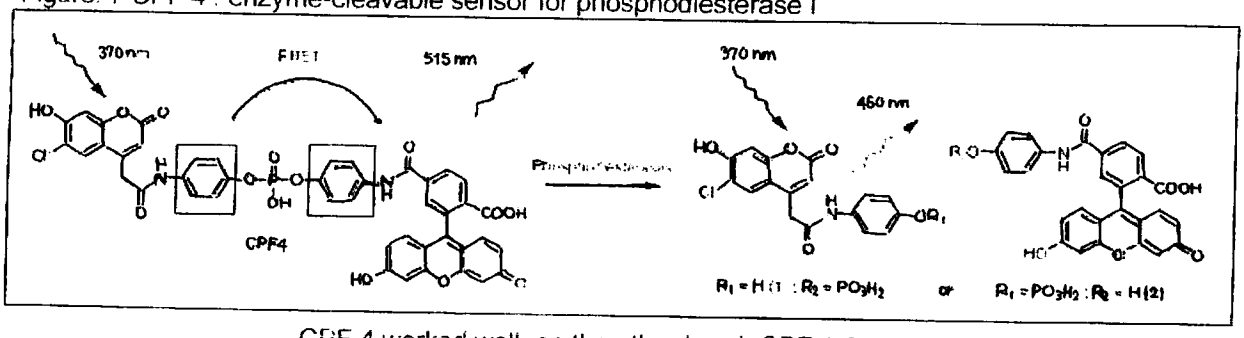

CPF 4 worked well, on the other hand, CPF 1-3.

Figure. 9 Sensors which did not show FRET or are not recognized by the enzyme

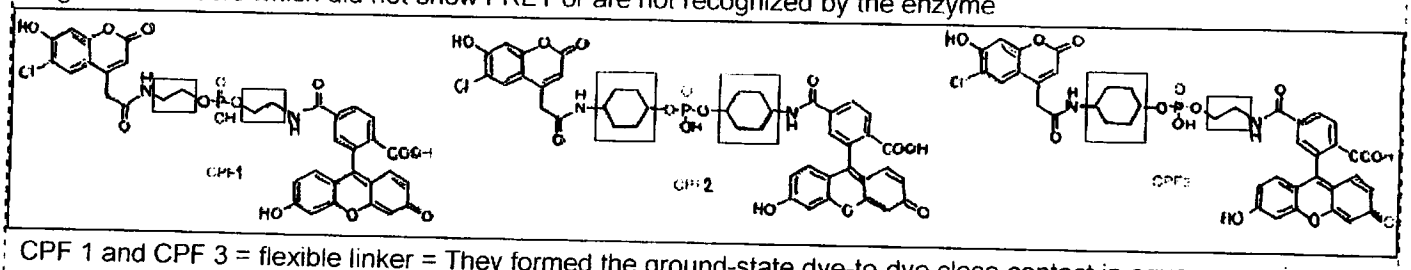

CPF 1 and CPF 3 = flexible linker = They formed the ground-state dye-to-dye close contact in aqueous environment (because fluorophore are hydrophilic. *cf.* In MeOH, they didn't do so.) then, fluorescence was quenched and FRET was not observed.

CPF 2 = rigid linker = It showed FRET.
(Excitation of the coumarin fluorophore resulted in increase of emission of fluorescein.)
But CPF 2 was not hydrolyzed by phosphodiesterase probably because of steric hindrance.

*quench = a decrease in quantum yield.
It can be caused several reasons.
In this case, two chromophores binded to each other *via* weak interaction before excitation, then formed non-fluorescent complex as a whole.

Phenyl linker has appropriate rigidity.

Figure. 8 Spectral profile of CPF 4

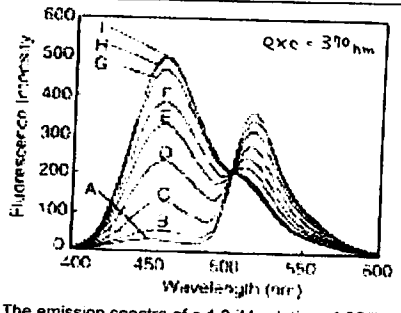

Figure 8. The emission spectra of a 1.0 iM solution of CPF_4 in Tris-HCl buffer (100 mM, pH 8.8) at 37 ℃: (A) without enzyme; (B) 1 min; (C) 5 min; (D) 10 min; (E) 15 min; (F) 20 min; (G) 30 min; (H) 45 min after addition of 0.05 u of phosphodiesterase I (Crotalus adamanteus venom); (I) a mixture of 1.0 iM 1 and 1.0 iM 2.

+ Figure. 10 (a)
As time goes by, blue-colored fluorescence from a corresponding coumarin emission band centered at 464nm decreased, and green-colored fluorescence from a fluorescein emission band at 517nm increased. This is consistent with increased FRET from the coumarin donor to the fluorescein acceptor.
+ Generation of open fluorescein was confirmed by HRMS.
+ Figure. 10 (b)
highly H_2O_2 selective
+ Figure. 10 (c)
application to yeast mitochondria H_2O_2 level detected RPF1(0.2uM) are within ranges reported using other analytical technique.

Figure. 10 Profile of RPF1

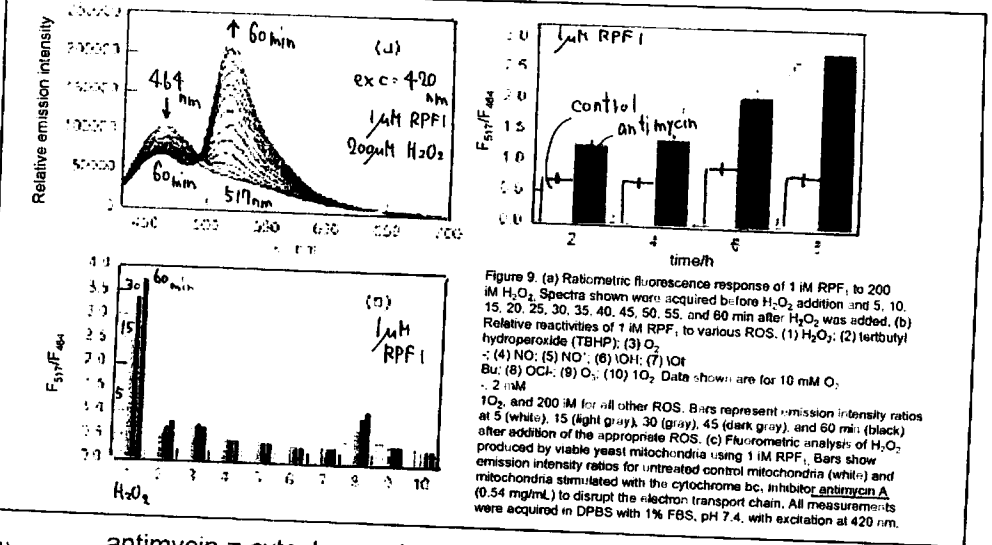

Figure 9. (a) Ratiometric fluorescence response of 1 iM RPF_1 to 200 iM H_2O_2. Spectra shown were acquired before H_2O_2 addition and 5, 10, 15, 20, 25, 30, 35, 40, 45, 50, 55, and 60 min after H_2O_2 was added. (b) Relative reactivities of 1 iM RPF_1 to various ROS. (1) H_2O_2; (2) tertbutyl hydroperoxide (TBHP); (3) O_2^-; (4) NO; (5) NO^-; (6) $^{\cdot}OH$; (7) $^{\cdot}OtBu$; (8) OCl^-; (9) O_3; (10) $^1O_2$. Data shown are for 10 mM O_2^-, 2 mM $^1O_2$, and 200 iM for all other ROS. Bars represent emission intensity ratios at 5 (white), 15 (light gray), 30 (gray), 45 (dark gray), and 60 min (black) after addition of the appropriate ROS. (c) Fluorometric analysis of H_2O_2 produced by viable yeast mitochondria using 1 iM RPF_1. Bars show emission intensity ratios for untreated control mitochondria (white) and mitochondria stimulated with the cytochrome bc, inhibitor antimycin A (0.54 mg/mL) to disrupt the electron transport chain. All measurements were acquired in DPBS with 1% FBS, pH 7.4, with excitation at 420 nm.

antimycin = cytochrome bc_1 inhibitor
= trigger generation of H_2O_2 and other reactive oxygen speices

+ visible wave length = minimize damage to sample

3. FRET-based investigation of conformational change : AMPA receptor

ref. G. Ramanoudjame *et al. Proc. Natl. Acad. Sci. USA* **2006**, *103*, 10473.

3.1 design concept of this work

FRET is induced when donor and acceptor get close by conformational change of protein.

1. large spectral overlap **2. distance (10 ~ 100Å)**
3. appropriate dipole orientation (κ^2 is not zero.)

In this work, protein is AMPA receptor (ligand-gated ion channel), and trigger is its ligands, or AMPA, glutamate and kainate.

Figure. 11 FRET induced by conformational change

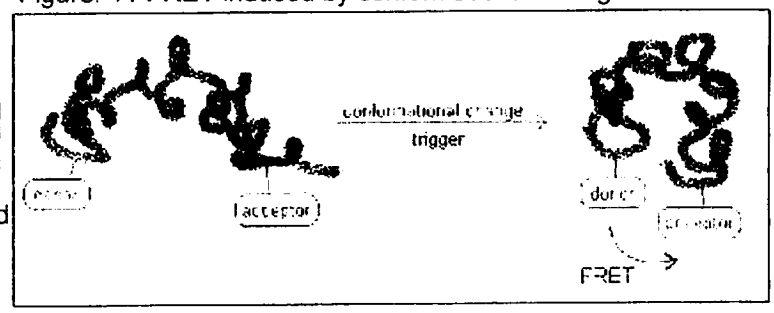

3.2 background

ref. E. Gouaux *et al. Nature* **2002**, *417*, 245.
E. Gouaux *et al. Proc. Natl. Acad. Sci. USA* **2003**, *100*, 5736.

Figure. 12 Receptor-AMPA complex

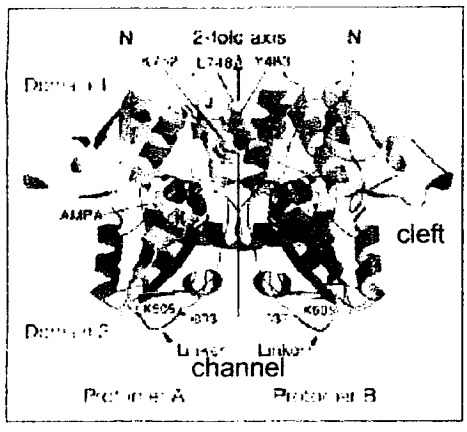

Figure. 13 A model for activation

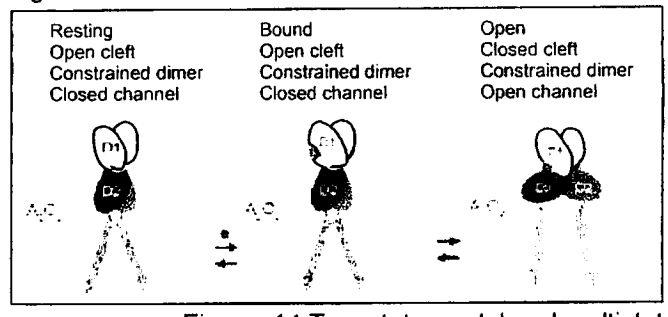

Figure. 14 Two-state model and multistate model

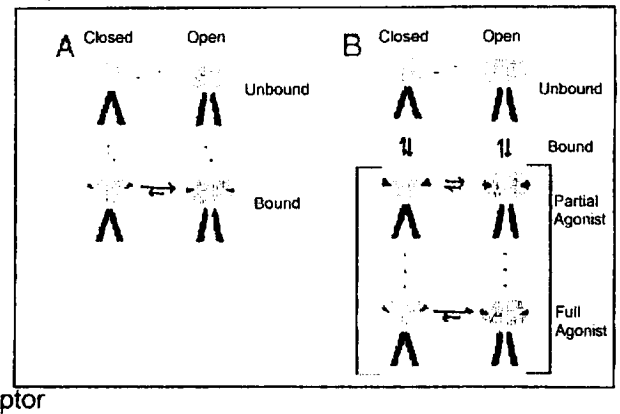

+ AMPA receptors : primary mediators of fast excitatory synaptic transmission in the mammalian CNS.
+ AMPA is a **ligand-gated ion channel** (Figure. 12, 13).
+ **Crystallographic analysis** showed that the extent of cleft closure in the ligand-binding domain controls the activation of the receptor (Chart. 1, Figure. 14).

Chart. 1 Cleft closure-activation correlation of **WT** AMPA receptor

AMPA and glutamate	**(full agonist)** : induced large cleft closure : **well-opened** channel
kainate	**(partial agonist)** : induced small cleft closure : **not well-opend** channel (multistate model)

correlation

+ L650T mutant

1. AMPA is a partial agonist in the context of L650T.
2. **AMPA**-bound form of the L650T mutation of the receptor **crystallized in two forms** ; one structure where the cleft is closed 11° and a second structure in which the cleft is closed 22° relative to the open apo form of the protein.

⇨ Intermediate activation by AMPA in this mutation is dictated by an equilibrium of a low-activity and high-activity state ?

These backgrouds were collected with crystallographic analysis.

Figure. 15 Activation profile of WT and L650T

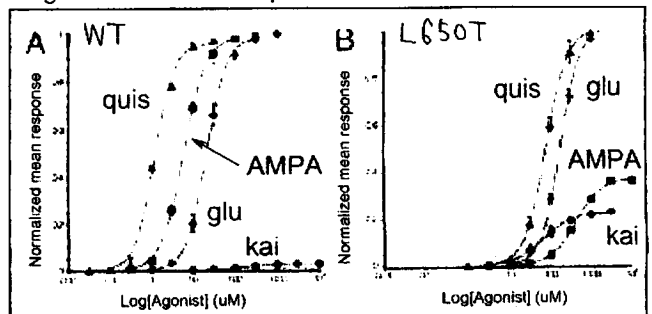

Fig. 2. Dose.response curves and Imax traces for the $L_{483}Y$ and $L_{483}Y_1$ $L_{650}T$ variants of the full-length $GluR_2$ receptor recorded by using the twoelectrode, voltage.clamp technique. (A) Normalized dose.response curves for glutamate (Glu) (), AMPA( ), quisqualate (Quis) (OE), and kainate (KA) (F) measured from oocytes expressing $GluR_2$ $L_{483}Y$ receptors. (B) EC_{50} data for the $GluR_2$ $L_{483}Y_1$ $L_{650}T$ mutant, in combination with glutamate (), AMPA ( ), quisqualate (OE), or kainate (F), scaled for efficacy relative to glutamate.

In this work, FRET-based assay allowed authors to investigate the conformational changes in the ligand-binding domain **in solution** without the crystallographic constrains.

3.3 fluorophore labeling

Two strategies were used.

Table. 1 Two strategies used

strategy	donor	acceptor
1	S652C-[DTPA-Tb]	His tag-[Cy3 derivative of nitrotriacetic acid chelate of Ni(II)]
2	S652C- [DTA-Tb]or[TTHA-Tb]	T394C-fluorescein

+ DTPA-Tb (DiethyleneTriaminePentaAcetic acid chelate of Tb) ref. *Annu. Rev. Biophys. Struct.* **2002**, *31*, 275.

* Antenna : absorb the excitation light then transfer the energy (because of weak absorbance of the lanthanide)
* Chelate : binding lanthanide tightly
  shielding the lanthanide ion from the quenching effects of water
  scaffold for the attachment of the antenna and a reactive group
* Lanthanide : Tb, Eu, Dy, Sm (emission in the visible region)

Figure. 16 Position of fluorophores

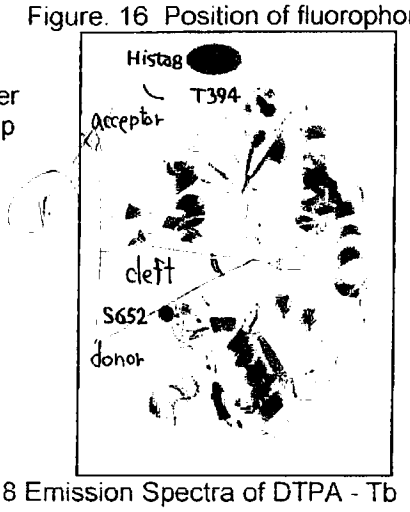

Figure. 17 Schematic illustration of DTPA - Tb donor

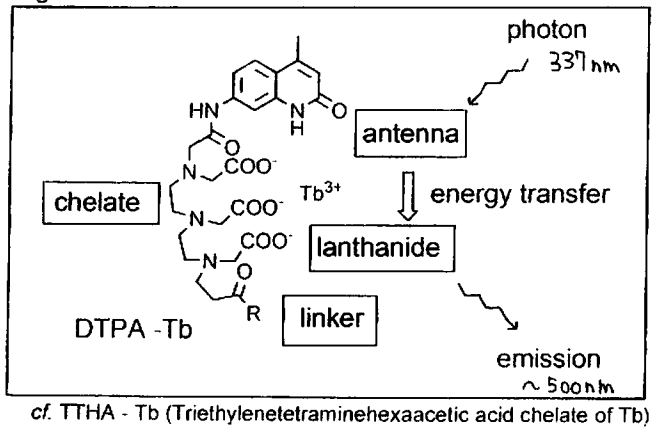

cf. TTHA - Tb (Triethylenetetraminehexaacetic acid chelate of Tb)

Figure. 18 Emission Spectra of DTPA - Tb

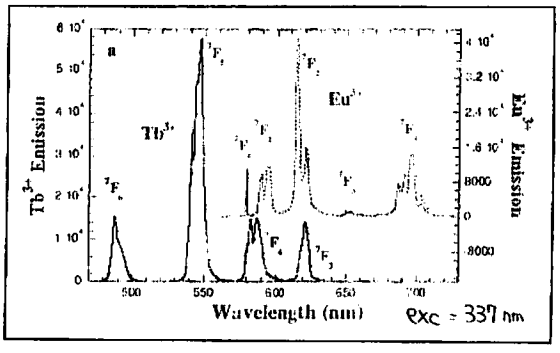

Characteristics
* large stokes shift
* sharply spiked emission (10-20nm)
* long excited-state lifetimes (msec) *cf.* organic dyes : nsec

⇩

advantage = discrimination against excitation light
eliminate background fluorescence

+ Cy_3 derivative of nitrotriacetic acid chelate of Ni(II) ref. *J. Am. Chem. Soc.* **2001**, *123*, 12123.

* labeling of protein : general use of cystein residue
* proteins that do not contain cystein residue : site-specific mutagenesis
* However, most proteins contain several cystein residues
  : site-specific labeling is difficult.

⇩

use of hexahistidine tag

The hexahistidine tag is known to interact tightly with transition metal complexes.

Figure. 19 Schematic representation of the mode of interaction

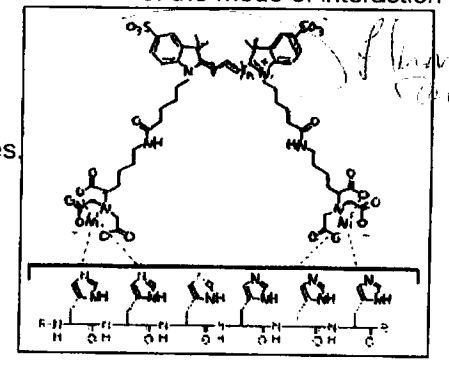

advantage

* widely used hexahistidine tag (purification, easy introduction etc..)
* in situ labeling

Figure. 20 1:1 stoichiometry between Ni(II)-NTA and His_6

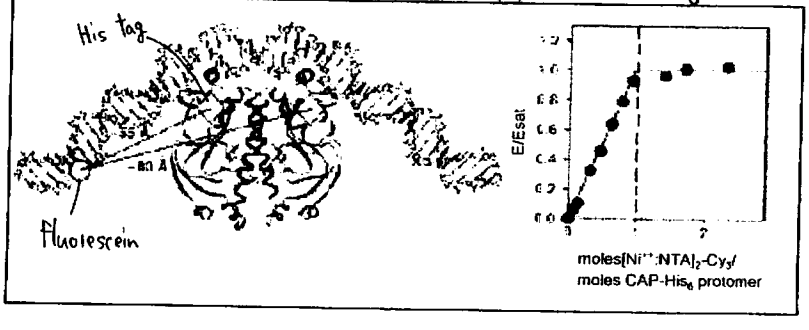

stoichiometry is 1:1.

3.4 conformational change analysis using wild type receptor

3.4.1 There is no accesible cystein in the interior of the protein

S652C protein was labeled with a 1:1 ratio of DTPA-Tb and fluorescein. (note that T394 was not mutated)

↓

no FRET observation

(This experiment provided proteins labeled by donor only or acceptor only at the accessible S652C residue.)

↓

no accesible cystein in the interior of the protein

Figure. 21 Fluorescence lifetime for S652C labeled with fluorescein and DTPA-Tb in the apo state

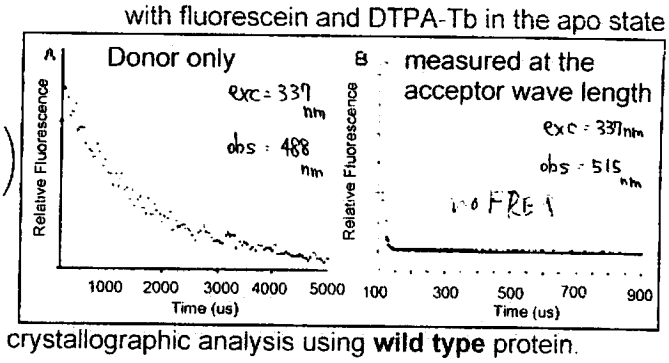

3.4.2 FRET study in solution supports the results obtained by crystallographic analysis using **wild type** protein.

The fluorescence lifetime of donor in the absence of an acceptor and FRET lifetime as mesured at the acceptor emission wave length were investigated.

↓

donor only lifetime : no significant difference regardless of ligands

FRET lifetime(acceptor) : AMPA = glutamate < kainate < apo

↓

$E = 1 - \frac{\tau_{AD}}{\tau_D}$ τ_{AD} : FRET lifetime of acceptor, τ_D : lifetime of donor only

↓

FRET efficiency : apo < kainate < AMPA = glutamate

↓

cleft closure : AMPA = glutamate < kainate < apo

(close) ⟶ (open)

This is consistent with the result of crystallographic analysis.

Figure. 22 Fluorescence lifetime : correlation between cleft closure and agonists

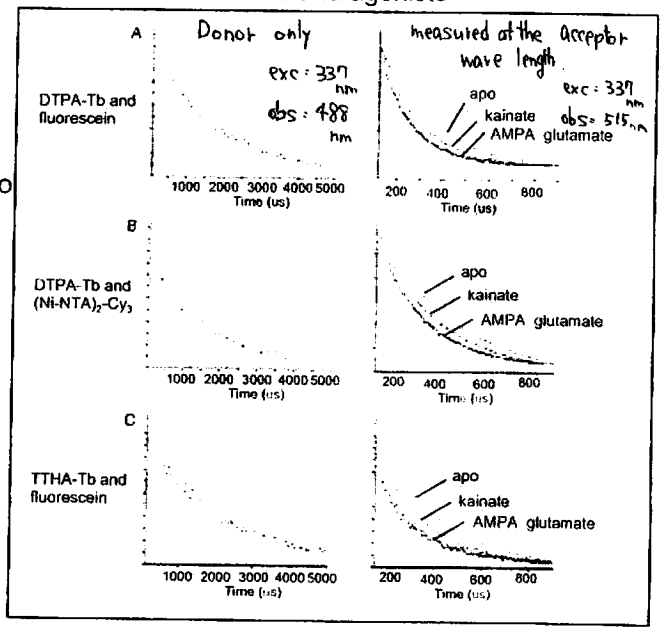

Figure. 23 Activation measured with voltage-clamp method

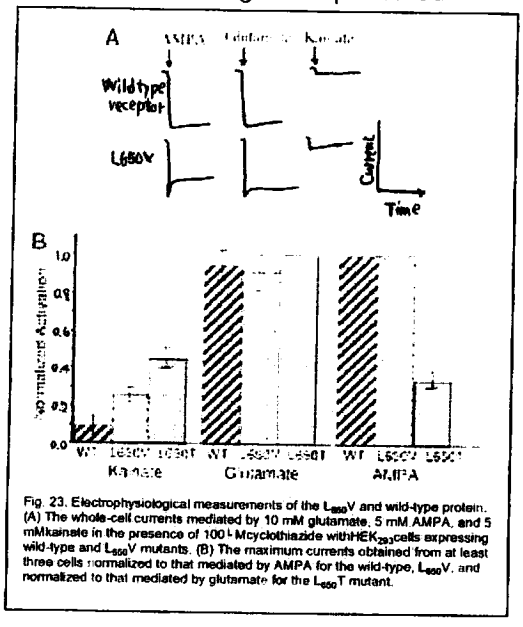

Fig. 23. Electrophysiological measurements of the $L_{650}V$ and wild-type protein. (A) The whole-cell currents mediated by 10 mM glutamate, 5 mM AMPA, and 5 mMkainate in the presence of 100 L-Mcyclothiazide withHEK$_{293}$cells expressing wild-type and $L_{650}V$ mutants. (B) The maximum currents obtained from at least three cells normalized to that mediated by AMPA for the wild-type, $L_{650}V$, and normalized to that mediated by glutamate for the $L_{650}T$ mutant.

Figure. 24 Activation-Distance relationships

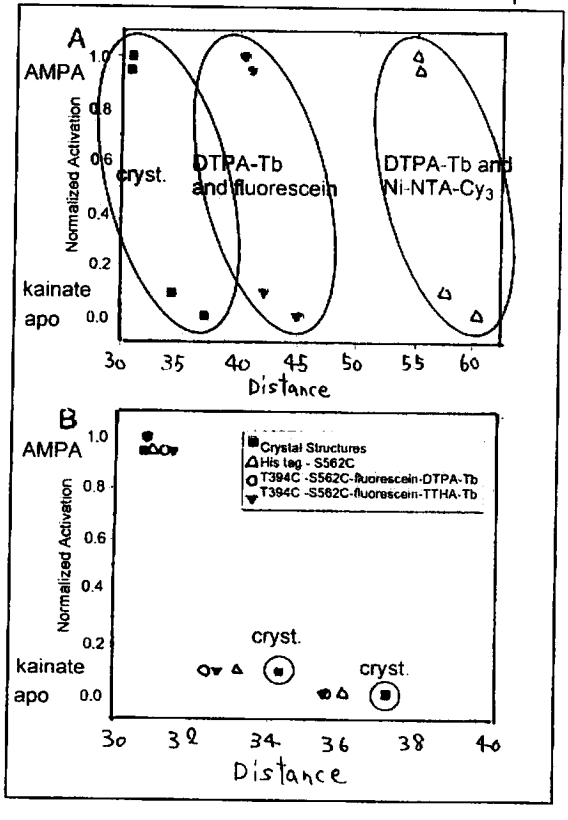

* relationships between distance measured with FRET and activation measured with voltage-clamp method

↓

6/10

The absolute distance differed, however the **changes** in distances between the various ligated states showed roughly good agreement.

↓

Minutely, distance changes of FRET study were smaller than those of crystallographic study.

Table. 2 Comparison of distance changes (Å)

	apo - kainate	kainate - AMPA
crystallography	3	7
FRET	3	5

3.4 conformational change analysis using L650T mutant receptor

The fluorescence lifetimes of L650V (control) and L650T were measured using the same method as wildtype.

↓

L650V followed the same trend as WT.
Unexpectedly, L650T also did so.

↓

AMPA, a **partial agonist** of this mutant protein, exhibited **larger ceft closure on average**.

+

FRET lifetime did **not** require a two-exponential fit.
= Two distinct populations were not present.

↓

Second conformation observed in the crystal structure of the AMPA-bound form of the L650T (11° cleft closure) is not a major second conformation.

↓

Low activation of AMPA in the L650T mutation is **not** due to an equilibrium of two distinct low- and high-activity confromations.

Figure. 25 FRET lifetime of L650V and L650T

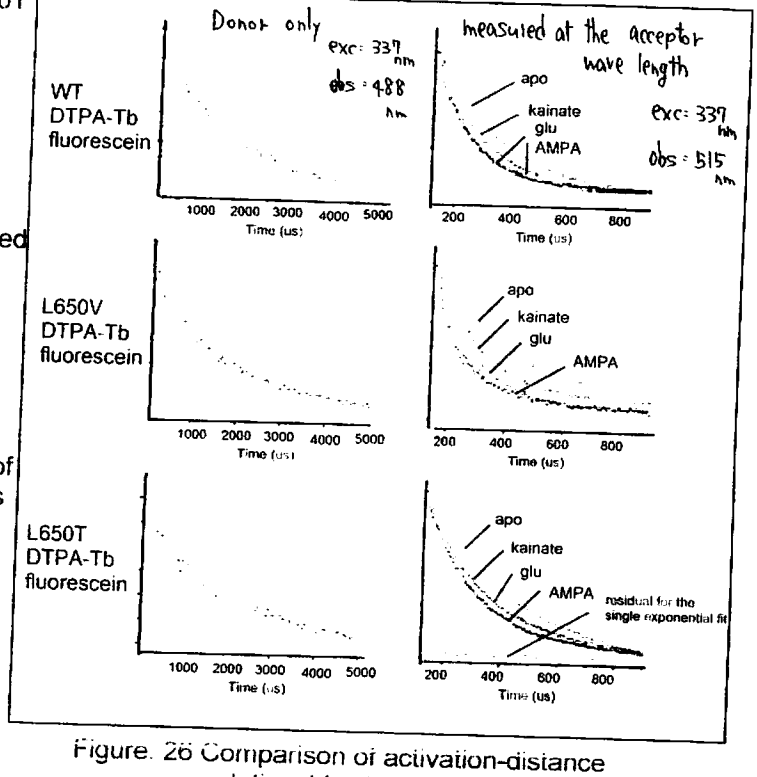

Summary

Although cleft closure is required for channel activation in the mutant, the subtle differences in the extent of activation does **not** necessarily have to be controlled by the degree of cleft closure.

Figure. 26 Comparison of activation-distance relationships between WT, L650V, L650T

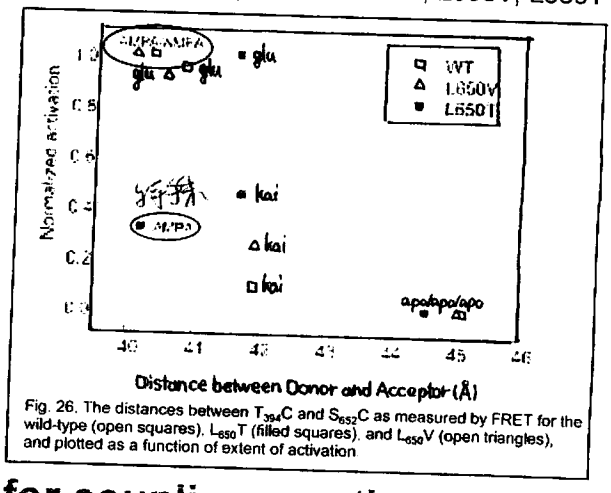

Fig. 26. The distances between $T_{394}C$ and $S_{652}C$ as measured by FRET for the wild-type (open squares), $L_{650}T$ (filled squares), and $L_{650}V$ (open triangles), and plotted as a function of extent of activation

existence of some other mechanism ?
such as direct coupling mechanism between agonist-binding domain and the channel segments through domain 2.

(see Figure. 13. In conventional mechanism, domain 1 is affected by ligand-binding and this effect is conveyed to cleft closure and in the next place to channel.)

4. FRET-based high-throughput assay for coupling reaction : Amination of aryl halide

4.1 purpose of this work

ref. J. H. Hartwig *et al. J. Am. Chem. Soc.* **2003**, *125*, 6977.

1. evaluate the accuracy of the FRET assay using palladium catalyzed amination of aryl halide as one case.
2. reveal whether high yield could be obtained with bases weaker than NaO*t*-OBu in more polar media than arenes and ethers using FRET assay. (more polar soivent has an advantage in that it can be used for pharmaceutical intermediates that are often insoluble in aromatic and ehter solvents.)

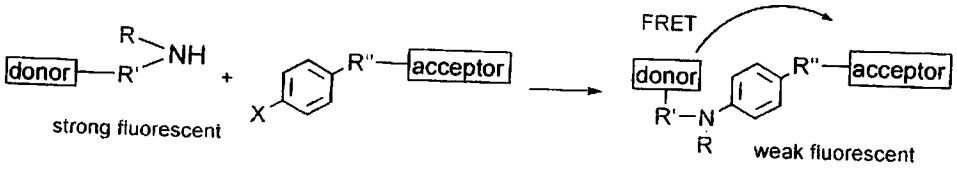

4.2 design and selection of chromophores

requires a donor and an acceptor that are stable to the basic conditions of the amination process.

Figure. 27 FRET pair

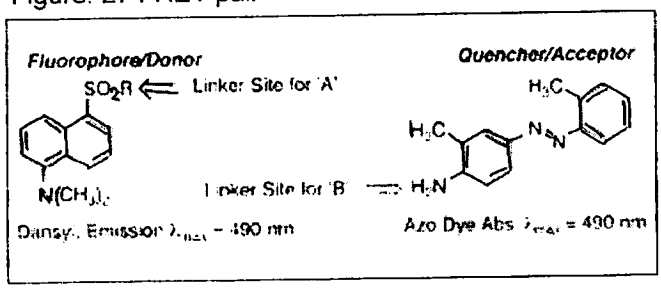

Figure. 28
Amine substrate **3**

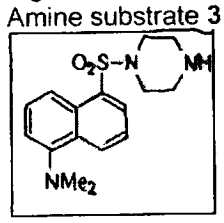

Figure. 29
Aryl halide substrate

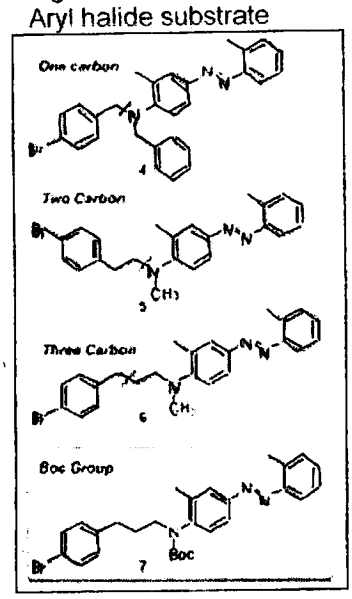

* **4**, **5**, and **6** underwent partial to complete cleavage of a carbon-carbon bond of the tether under the reaction condition (3mol% $Pd(OAc)_2$, 2.8mol% $(t\text{-}Bu)_3P$), 1.5eq. NaO*t*-Bu, 80°C.
* They used substrate **7** and its chloride analogue for further studies.

4.3 calibration curve

Solutions containing various ratios of coupled product **8** and starting materials **3** and **7** (1:1 ratio) were prepared, and the fluorescence intensities of the solutions were measured

Table. 3 Preparation of calibration curve

Vials	Stock A (uL)	Stock B (uL)	Emission Intensity	Mole Fraction of Coupled Product 8
1	20	0	61621	0.0
2	16	4	51158	0.2
3	12	8	37826	0.4
4	8	12	25465	0.6
5	4	16	13176	0.8
6	0	20	2936	1.0

Figure. 30 Calibration curve

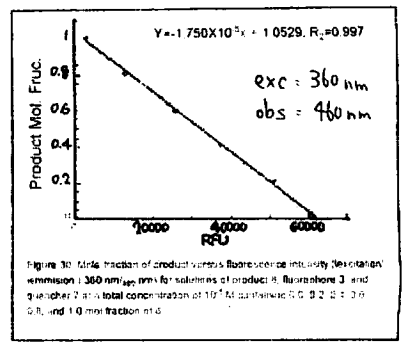

4.4 screening the reaction of dansylpiperazine 3 with bromoarene 7

The reactions were conducted in a 96-well glass plate with 50μl volumes.
* CpPd(allyl) was used instead of $Pd(OAc)_2$ as catalyst precursor because of its enhanced solubility. ($Pd(OAc)_2$ was used for imidazolium and dihydroimidazolium salts.)

119-membered ligand library
duplicate reaction with each member of the ligand library.

Figure. 31 Yields determined by FRET for the coupling of **3** with **7**

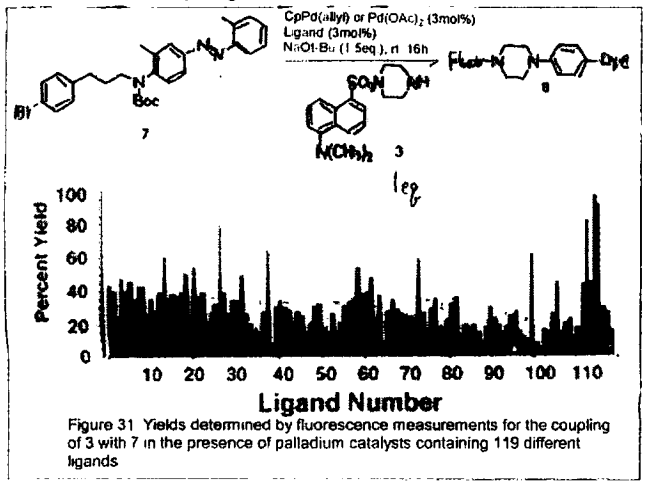

Figure 31 Yields determined by fluorescence measurements for the coupling of 3 with 7 in the presence of palladium catalysts containing 119 different ligands

Figure. 32 General structural classes contained in the library

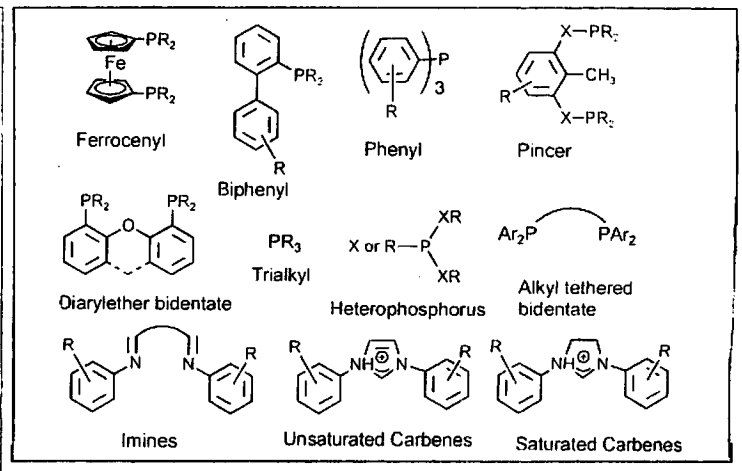

Figure. 33 shows the structures of the ligands that consistently generated catalysts that formed coupled product in yields greater than 50%.

These results were in accord with studies over the past few years.

*Two false positives (***L59** and ***L106***)

They tested the activity of ***L59*** and ***L106*** for the related reaction of morpholine with bromotoluene (not functionalized with chromophore), because structures of these ligands were much different from others shown to be active.

L59 gave 12% yield, and ***L106*** gave 0% yield.

people assesment is necessary.

Figure. 33 Ligands that gave >50% yield for the coupling of **3** with **7**.

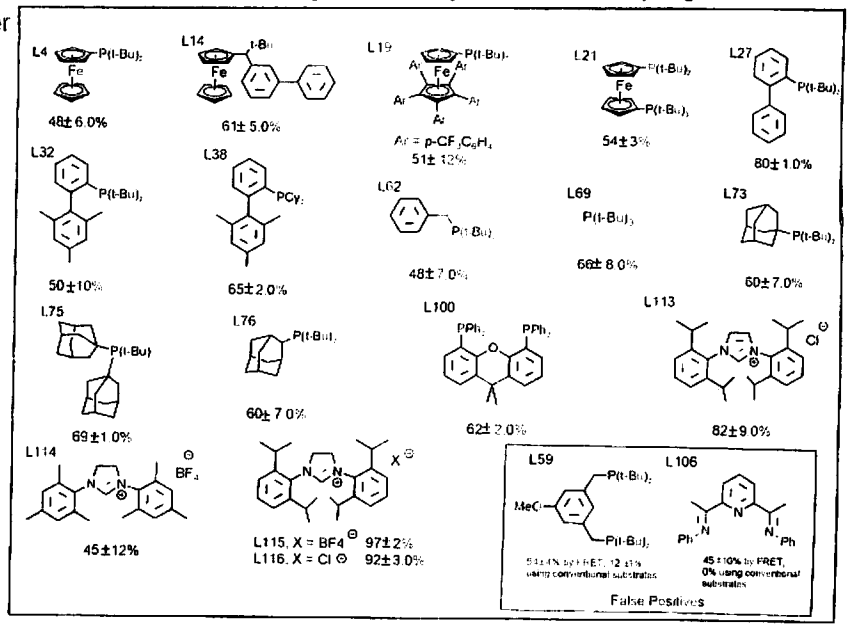

4.5 screening the reaction of dansylpiperazine 3 with chloroarene 9

Figure. 34 Yields determined by FRET for the coupling of **3** with **9**.

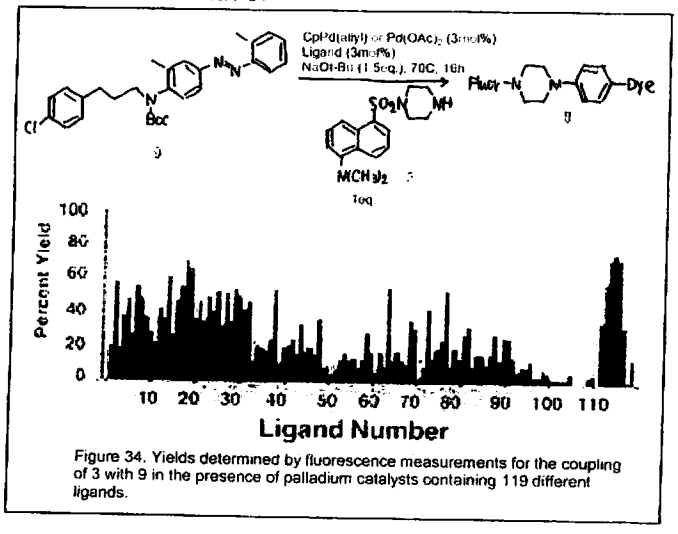

These results are also in accord with those of recent studies.

Only a few reactions showed significant variability in yields for the two experiments, however these reactions occurred in less than 20% yield.

Figure. 35 Ligands that gave >50% yield for reaction of **3** and **9**.

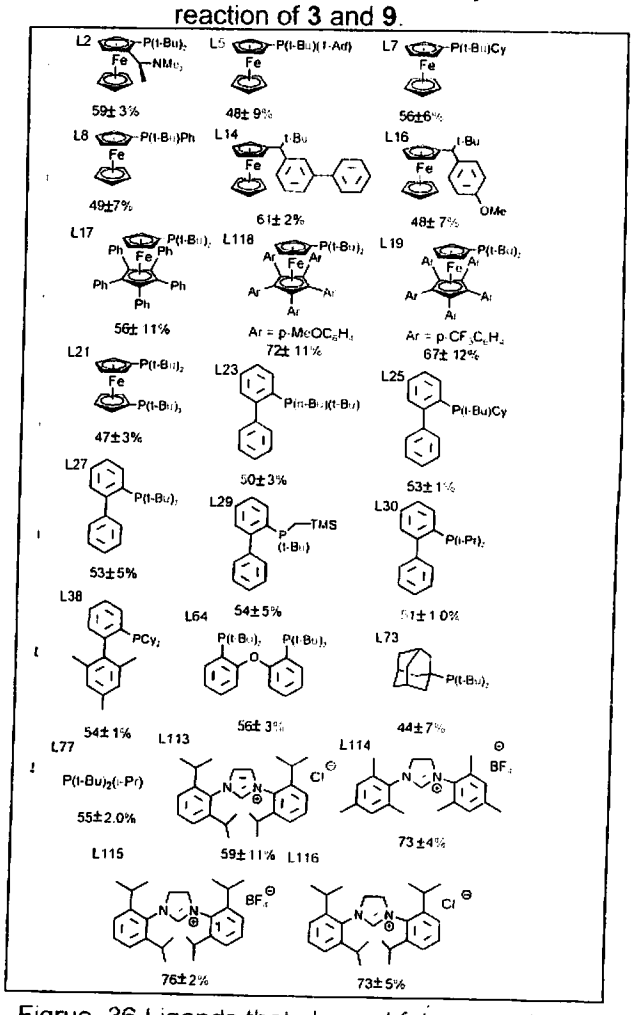

4.6 investigation of potential false negatives

Catalysts containing ligands shown on the right are known to couple electron neutral aryl chlorides and bromides with cyclic secondary amines in yields greater than 80%.

false negative

Figrue. 36 Ligands that showed false negative

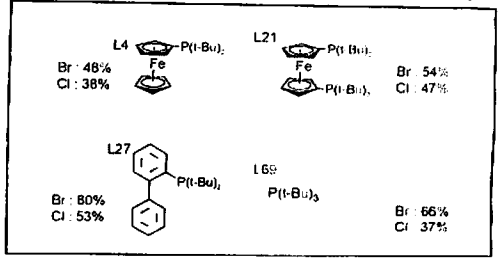

To confirm that these ligands provide high yield for related substrates under the conditions of the FRET assay, they evaluated the reaction of bromotoluene with morpholine in the presence of CpPd(allyl) and $(t\text{-Bu})_3P$ (***L69***).

⟶ 98 % yield by GC after 16h

↓

What is the origin of low yields in the FRET assay ?
the method of analysis ? or substrate ?

↓

They conducted three reactions.

1. determination of yield with ^1H NMR (substrate = **3** and **7**)---------- 60%
2. reaction of morpholine with functionalized bromoarene **7**. ---------- 64%
3. reaction of functionalized amine **3** with bromotoluene. ---------- 95%

↓

FRET study evaluated the yields accurately.
(The reason of low yields is substrate **7**, not the method of FRET analysis)

Figure. 37 Model reaction

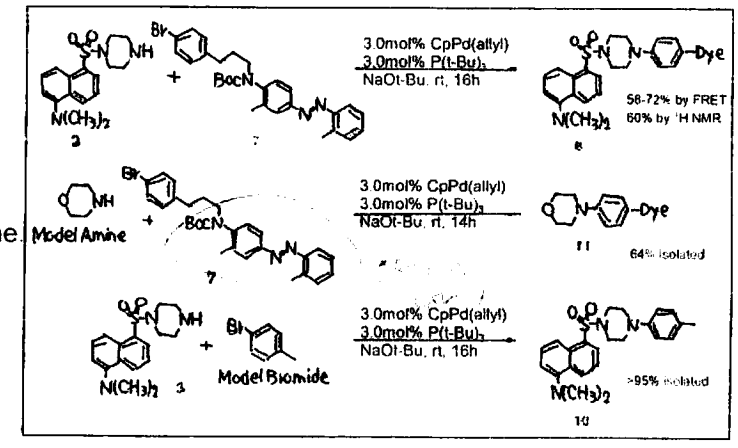

4.7 reaction of amine 3 with bromoarene 7 in polar solvents with K_3PO_4 as base

Using polar solvent is advantageous because in particular pharmaceutical intermediates are often insoluble in aromatic and ether solvents.

↓

dioxane/*m*-xylene or *t*-BuOH/*m*-xylene gave good results.

Figure. 38 Solvent screening

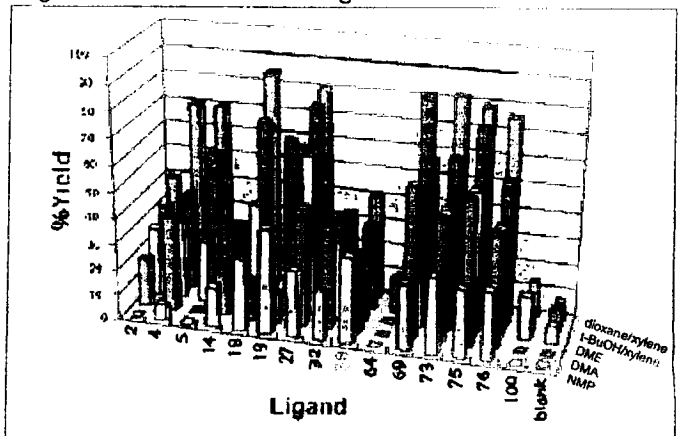

Figure 38. Yields determined by FRET for the reaction of 3 with 7 at 80 ℃ for 16 h in the presence of K_3PO_4 as base

Summary

FRET can be used to screen catalyst and solvent for the *amination of aryl* halides and by analogy, to screen other catalysis via high-throughput manner. The reaction yields obtained by FRET method were reproducible and agreed in most cases with yields obtained by conventional methods.

5. Recent progress and perspective

+ Application to *in vivo* system (assay, sensor, etc..)
+ Development of new chromophore (quantum dot, gold nanoparticle, etc..)
+ Efforts toward extending distance which one can measure (multi FRET, new chromophore, etc..)
+ Development of methods for labeling

Applicable to developing a new reaction ?
* Hartwig : high-throughput (yield)
* design and synthesis of new catalyst

* ordinary C-C bond = 1.5Å(*cf.* FRET = 10 - 100Å)
* *fluorophore* is too big. (alter the characteristics of catalysts or so)

$R_0 = 9.78 \times 10^3[\kappa^2 n^{-4} Q_d J]^{1/6}$ (in Å) eq. 2

* exploring of a pair of fluorophores which give small R_0
* development of devices which can detect weak fluorescence
* small fluorophores

Figure. 39 dependence on distance